https://doi.org/10.14669/AM/192666

MODELING OF FULL VEHICLE DYNAMICS FOR ENHANCED STABILITY CONTROL

DONIYOR AKHMEDOV[1], DAVRON RISKALIEV[2]

Abstract

Dynamic models utilized for assessing vehicle stability typically possess a limited number of degrees of freedom, commonly known as a planar model. Simultaneous examination of vibration and stability is unfeasible within these models. Additionally, such models pose several challenges in terms of adaptation to emerging vehicle technologies, rendering them unsuitable for real-time control. Furthermore, the dependability of outcomes derived from dynamic systems with limited degrees of freedom remains uncertain. This article presents a theoretical and experimental comparison analysis of a dynamic model designed to assess the vibration and motion stability of a vehicle with twelve degrees of freedom. The empirical investigations were conducted under actual road conditions, employing a four-step approach: horizontal vehicle model, vertical vehicle model, liner tyre model, and driver model. The experiment shows that a error was close to 15% when the speed of movement increased from (75–80) km/h in the 12DOF model, likely due to the linearity of the tire model. This is due to the non-linear elastics of the steering and suspension, as well as the kinematic introduction during the turn of the car. Based on the conducted research, it is recommended to use non-linear models of tires and suspensions in further studies.

Keywords: dynamic model; vehicle stability; vertical bicycle model; horizontal bicycle model; vertical model

1. Introduction

State-of-the-art computing technology and software packages provide comprehensive measurement and stabilization. The movement of the car on the road is determined by an equation set. Without software, the solution of these equations is subject to a number

[1] Automotive Engineering, University of Public Safety of the Republic of Uzbekistan, Uzbekistan, e-mail: emailyoshlik1982xonobod@gmail.com, ORCID: 0009-0009-6813-1094

[2] Automotive Engineering, Tashkent State Transport University, Uzbekistan, e-mail: davron.riskalievsh@tstu.uz, ORCID: 0009-0004-6453-6362

https://doi.org/10.14669/AM/192666

of assumptions that can have an impact on the reliability of the results. More accurate solutions to these problems can be achieved by using modern application packages such as MATLAB®/Simulink. This article focuses on the development of dynamic models with minimal assumptions to describe the horizontal, vertical and angular vibrations of a car. The resulting values allow the evaluation of the car's controllability and stability. To assess the suitability of the dynamic model developed, experimental studies were carried out under real road conditions. Comprehensive dynamic modeling of full vehicle dynamics plays a crucial role in enhancing stability control by considering various factors impacting tire force characteristics and overall vehicle behavior. By analyzing tire temperature, inflation pressure, and tread depth, models like the Pacejka 'magic formula' can be adapted to compensate for these variables [1, 2, 3]. Additionally, nonlinear vehicle dynamics models, integrating longitudinal and lateral dynamics, are utilized to predict vehicle states under extreme conditions, ensuring rapid adaptation to changing stability requirements [4, 5, 6]. These advanced modeling techniques enable the development of control strategies, such as model predictive control, that can effectively manage stability by dynamically adjusting control inputs based on real-time data, ultimately improving overall vehicle safety and performance.

The effectiveness of full vehicle dynamics stability control is influenced by various factors. These include the consideration of time delays in feedback control systems [7, 8], the integration of reliable control schemes to address actuator failures and external disturbances [9, 10], the complexity of vehicle dynamics and working conditions necessitating the utilization of nonlinear tire forces for improved chassis control strategies [9, 11], and the optimal use of control allocation methods to coordinate multiple actuators effectively for vehicle motion control [12]. Additionally, the establishment of stability judgment based on phase plane analysis and the development of stability controllers like direct yaw-moment control contribute significantly to enhancing stability control effectiveness [11]. By incorporating these factors, researchers aim to advance vehicle safety, comfort, and performance through sophisticated stability control systems.

2. Materials and Methods

Vehicle dynamics model. Vehicle dynamics models play a crucial role in various applications, including autonomous racing and passenger vehicle analysis. Studies have highlighted the significance of accurate vehicle dynamics models [15, 16]. These models typically involve multiple degrees of freedom to capture the complex behavior of vehicles during motion. For instance, dynamic vehicle models with seven degrees of freedom have been established to analyze driving vehicle behavior, considering aspects like sprung mass motion and unsprung masses. Researchers have explored different methods, such as Gaussian Process regression, to approximate vehicle dynamics models, emphasizing the balance between computational demands and model accuracy. These models aid in predicting a

https://doi.org/10.14669/AM/192666

vehicle's responses to various inputs, contributing significantly to vehicle design, simulation, and performance evaluation in both autonomous and traditional driving scenarios.

Different types of vehicle dynamics models vary in accuracy and applicability for predicting vehicle behavior. Physical modeling-based approaches, while simplistic, may lead to errors due to parameter approximations [6]. Model-based estimations like Kalman Filtering offer accuracy based on the model and estimation algorithm chosen [7]. Learning-based methods, such as Gaussian Process regression, aim to approximate vehicle dynamics for autonomous racing, but may lack realism [9]. Hybrid models combining physical and deep learning methods show lower error and higher interpretability compared to purely data-driven approaches [10]. Nonlinear dynamics models, like the multibody vehicle model, provide accurate real-time simulations for intelligent control in ADAS applications [11]. Each model type has its strengths and limitations, with a trade-off between complexity, accuracy, and computational efficiency based on the specific application requirements.

To examine the stability of a car, a comprehensive mathematical description of it as a regulated object in the system of road, tire, car, and driver is necessary. This system integrates mechanical vibrations of individual masses, such as the body and unsprung masses, with other physical processes that affect the movement characteristics of the vehicle. These processes include the interaction between the vehicle and the driver during controlled movement, the operation of vehicle control systems, and the interaction with the external environment and road surface. The full dynamic behaviour of the vehicle has been extensively studied in previous works [11, 12, 13]. The present paper uses a 14-degree-of-freedom dynamic model, where the wheel tire movements are reflected by a "black box". Correction coefficients are used in scientific studies to accurately measure the movement of tires in vehicle stability research [18, 20] and the behavior of the vehicle during the 'lane change' maneuver was investigated using the 'bicycle' model. However, such models do not account for tire roll-in angles resulting from vehicle suspension kinematics. Using the above analysis, the authors developed a dynamic model with 12 degrees of freedom.

2.1. Horizontal vehicle model

The modelling process was carried out step by step. Initially, the movement of the car in the horizontal plane was developed based on the calculation scheme presented in Figure 1.

https://doi.org/10.14669/AM/192666

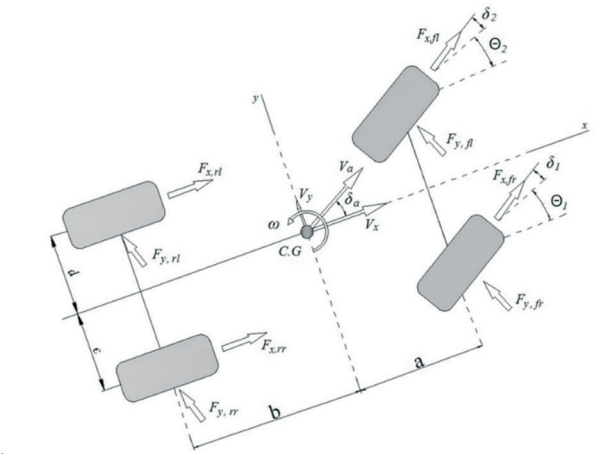

Fig. 1. Horizontal vehicle model

The movement of the car in the horizontal plane is characterised by three degrees of freedom: longitudinal movement (x-axis), lateral movement (u-axis) and rotational movement (z-axis) around its centre of gravity. The equations of horizontal motion for wheeled cars (see Figure 1) consist of three differential equations.

$$\begin{cases} M\ddot{x} = F_{x,fr} + F_{x,fl} + F_{x,rr} + F_{x,rl}; \\ M\ddot{y} = F_{y,fr} + F_{y,fl} + F_{y,rr} + F_{y,rl}; \\ I_z\dot{\omega} = a\left(F_{y,fr} + F_{y,fl}\right) - b(F_{y,rr} + F_{y,rl}) \end{cases} \tag{1}$$

M – vehicle total mass, kg
$\ddot{x}, \ddot{y}$ – longitudinal axis and lateral axis acceleration, m/s^2
F_x, F_y – longitudinal axis and lateral force at each tire, N
I_z – vertical axis moment inertia, kg·m^2
$\dot{\omega}$ – yaw angular acceleration, rad/s^2
a – distance between CG and the front axle, m
b – distance between CG and the rear axle, m
x,y – vehicle longitudinal and lateral position, m
v – vehicle velocity, m/s
v_x, v_y – vehicle longitudinal and lateral velocity, m/s
δ_a – vehicle side slip angle, angle between the vehicle center line and v, rad
δ_1, δ_2 – slip angle each tire, rad
fr, fl, rr, rl – the wheels are located in the front right-hand, front left-hand, rear right-hand and rear left-hand positions respectively.

https://doi.org/10.14669/AM/192666

2.2. Vertical vehicle model

At the second stage, we will establish the equations for the vertical, lateral and longitudinal vibrations of the car (Figure 2).

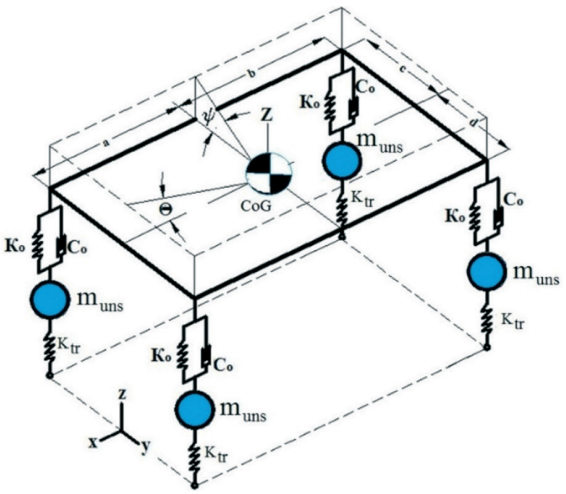

Fig. 2. Vertical vehicle model

When expanded, this system of equations has seven degrees of freedom. The given differential equation is in the following form:

$$\begin{cases} M_s\ddot{Z}_s = \sum P_s \\ I_y\ddot{\theta} = \sum M_y \\ I_x\ddot{\psi} = \sum M_x \\ \sum_{i=1}^{4} m_{uns,i}\ddot{Z}_{uns,i} = \sum_{i=1}^{4} P_{uns,i} \end{cases} \tag{2}$$

M_s – vehicle sprung mass, kg
$\ddot{Z}_s$ – vertical acceleration at sprung mass (CoG), m/s^2
ΣP_s – total vertical force at vehicle unsprung mass, N
I_x, I_y – longitudinal and lateral axis moment inertia, kg·m^2
ΣM_x, ΣMy – longitudinal and lateral axes total moments, N·m
Θ – vehicle pitch angle, rad
ψ – vehicle roll angle, rad
$m_{uns,i}$ – unsprung mass of the i-the wheels, kg
$\ddot{Z}_{uns,i}$ – vertical acceleration of the i-the wheels, m/s^2
$\Sigma P_{нп,i}$ – total vertical force acting on the sprung masses of the, N
K_{tr} – tire stiffness, N/m
K_0 – suspension stiffness, N/m
C_0 – suspension damping, Ns/m

https://doi.org/10.14669/AM/192666

2.3. Linear tire model

Developing a real dynamic tyre model is very difficult. In this research, we use the dynamic tyre model of [14] with minimal assumptions, which allows us to consider the inertia of the tyre and the lateral vibration of the car riding on the tyre. The first-order constraint equations are presented in the following form:

$$\begin{cases} Y_i = c_{tr,i}\xi_i \\ \frac{1}{v}\dot{\xi}_i + \frac{c_{tr,i}}{K_{yi}}\xi_i = -\delta_i \end{cases} \tag{3}$$

Y_i – horizontal lateral reaction, N
ξi – lateral tire deformation, m
$c_{tr,i}$ – tire lateral stiffness of the i-the wheels, N/m
K_{yi} – slip resistance coefficient, N/rad
δ_i – slip angle, rad
v – linear speed wheel, m/s
i – 1,2 (1 – for front wheel, 2 – for rear wheels).

2.4. Driver model

During the fourth stage, the impact of the driver and steering was assessed. The equations of motion of the steered wheels relative to the axis of rotation are expressed in the following form in the dynamic model of the steering wheel:

$$J_k\ddot{\Theta} = M_c + M_\lambda + c_p\left(\frac{\alpha}{i} + \Theta\right) \tag{4}$$

J_k – wheel moment of inertia, kg·m^2
M_c – moment is caused by the rolling of the wheel while the steering wheel moves in and out, N·m
M_λ – the moment of viscous friction is reduced to the axis of the steering wheel strut, N·m
c_p – steering stiffness, N/rad
α – steering wheel rotation angle, rad
i – steering ratio, numerical
Θ – steering angle, rad

2.5. Modular architecture of vehicle model

Based on these (1), (2), (3), (4) dynamic models, we build a simulation model in the Simulink environment. The architecture and communication algorithm of the simulation model is presented in Figure 3. Therefore, we obtain a dynamic model of the car with 12 degrees of freedom.

https://doi.org/10.14669/AM/192666

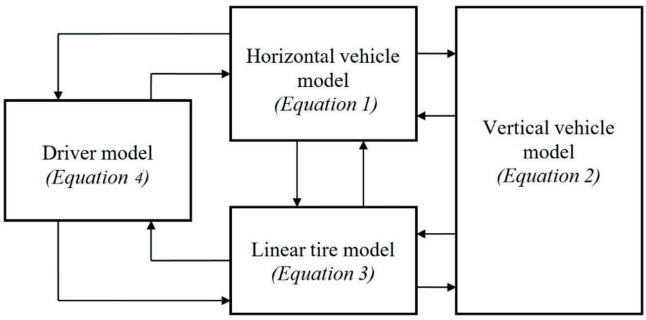

Fig. 3. Modular architecture of vehicle model

The model for studying the dynamic movement of the car was developed using Matlab/Simulink and is based on the scheme shown in Figure 3. An overview of the model is provided in Figure 4.

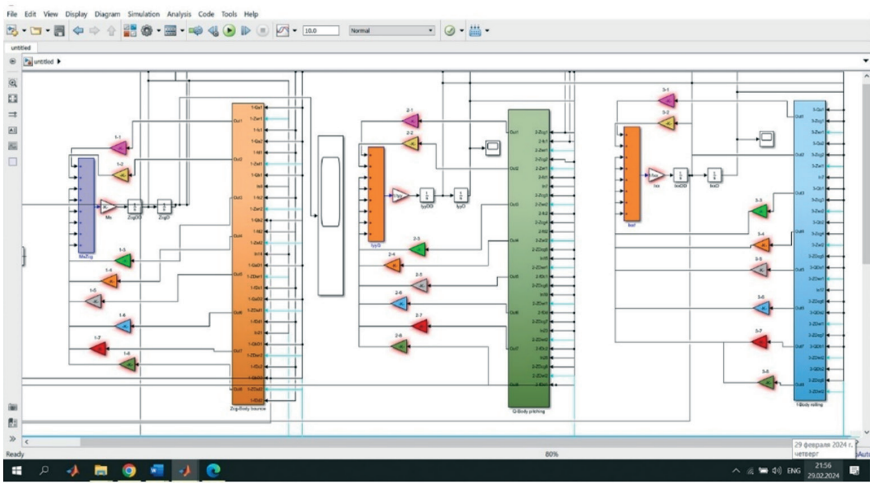

Fig. 4. This is a general overview of the subsystem used for simulation models in the Matlab/Simulink environment

3. Results

Modeling external signals in Matlab/Simulink can be complex. The authors created the [19] input signals for the steering wheel in Matlab/Simulink for J-turn and single lane change maneuvers, as shown in Figure 5.

https://doi.org/10.14669/AM/192666

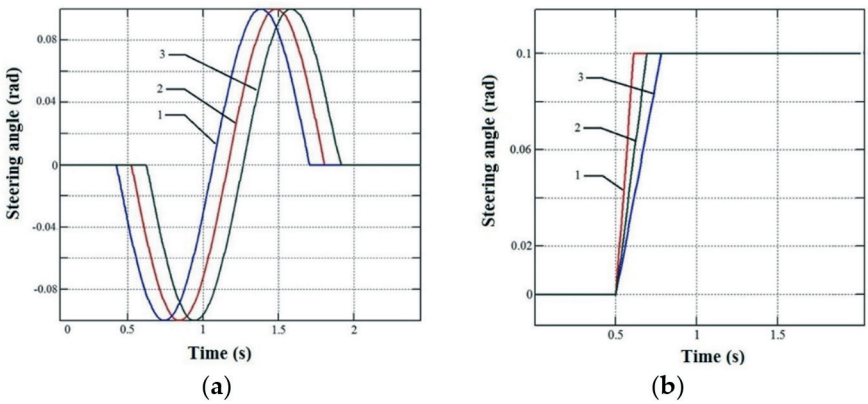

Fig. 5. Matlab/Simulink steering input signals for single lane change (a) and J-turn (b): 1,2,3 – The rotation intensity of the steering wheel at different frequencies

The aim of experimental research is to assess the suitability of the developed dynamic model. The tests were conducted using the 'J-turn' and 'Single lane change' maneuvers (Figure 6), which were selected based on the test methods outlined in the international standard [15–17].

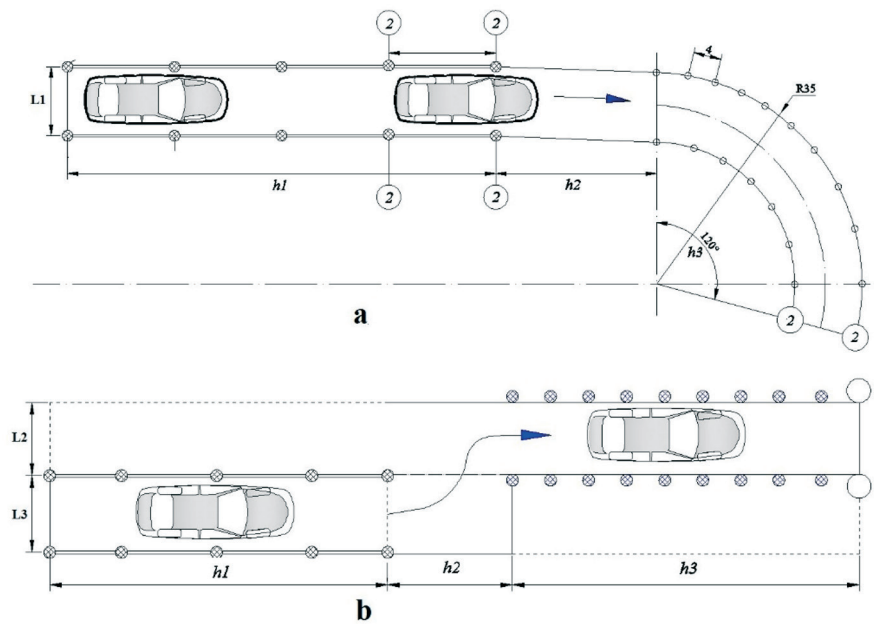

Fig. 6. J-turn (a) ва single lane change (b) maneuvering scheme: L1, L2, L3, h1, h2, h3

https://doi.org/10.14669/AM/192666

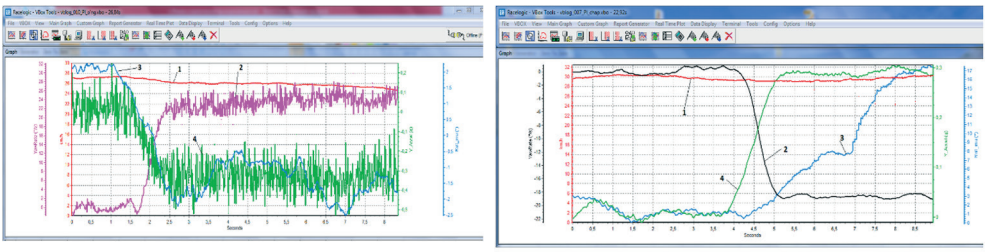

(a) (b)

1–vehicle speed; 2–angular speed of the car; 3–body roll; 4–lateral acceleration of the car.

1–vehicle speed; 2–angular speed of the car; 3–body roll; 4–lateral acceleration of the car

Fig. 7. Real test results of J-turn maneuver

The experiment utilised a device comprising a motion sensor, accelerometers, and other measuring instruments. The motion sensor has the following capabilities: a dynamic range of ±450 0/s for angular velocity measurement, a measurement error of 0.01% across the full range, a 16 bit ADC with a capability of 0.014 0/s, a displacement stability of ±0035 0/s, and a conductivity characteristic of 50 Hz.

The accelerometer records lateral, longitudinal, and vertical accelerations. It has a measurement range of ±5 g, a measurement error of 0.03%, and a 16-bit ADC (0.15 mg) sensor. The voltage range of the consumer current is (7–30) V, and it operates within a specific temperature range.

The car underwent tests at speeds of 30 km/h, 50 km/h, and 70 km/h. The initial tests involved driving over artificial bumps with h1=8 cm and h2=12 cm, and recording the resulting vertical vibrations. Subsequently, the car was tested in J-turn (a) and single lane change maneuvers. Figure 7 shows some of the test results in J-turn mode.

The vehicle, road, and external signal parameters were modelled using Matlab/Simulink. This included car weight (900–1400 kg) without passengers and with 4 passengers, speed ranging from 30 km/h to 70 km/h, and tire rolling resistance coefficient of (30000–40000) N/rad, among other variations.

Figure 8 illustrates the vibration of the vehicle body (sprung mass) over a single bump (a) and the vibration of the body along the longitudinal axis (b). The results of Vertical BM – 3 degrees of freedom 'vertical bike model', 12 degrees of freedom full model '12DOF' and real experiment are presented.

https://doi.org/10.14669/AM/192666

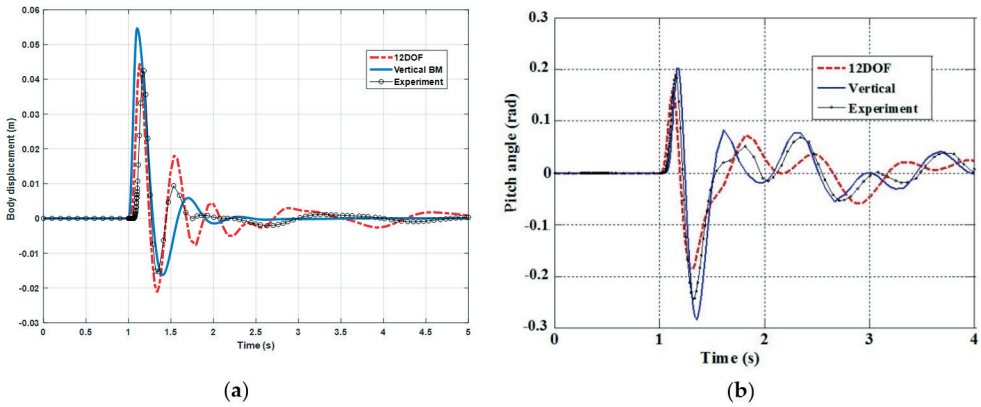

(a) (b)

Fig. 8. Body displacement (a) and pitch angle (b) results

Figure 9 illustrates the results stemming from a solitary lane alteration. The utilization of the dynamic model 'BM', characterized by 2 degrees of freedom and motion within the horizontal plane, facilitated the acquisition of outcomes at a consistent velocity.

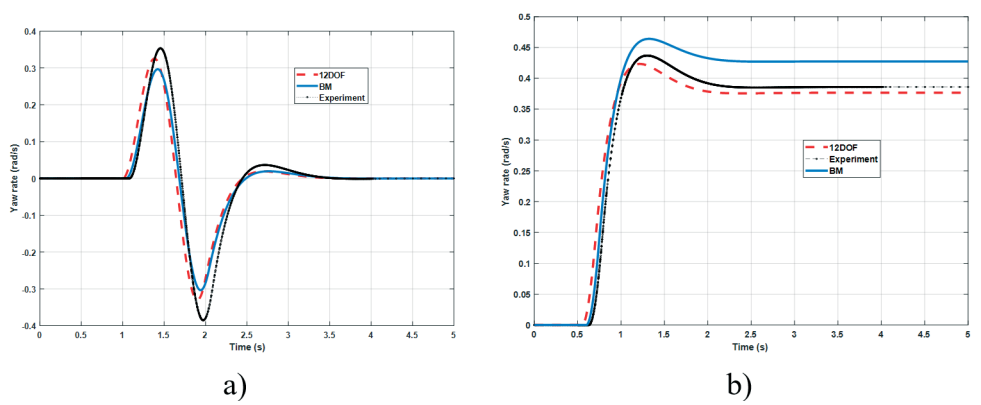

a) b)

Fig. 9. Single lane change (a) and J-turn (b) results

After the comparison of experimental results, we compared 12DOF, Vertical BM and BM with each other, and in our further studies we only compared theoretical studies.

The results (Figure 10) of a vehicle performing a single lane change at a speed of 20 m/s. The graph in Figure 10b compares the difference between the 12DOF and BM models by plotting the difference of values at each current time.

https://doi.org/10.14669/AM/192666

Figure 11 illustrates a J-turn manoeuvre modelled with a vehicle travelling at a speed of 20 m/s on a lane with a radius of 50 m.

Figure 12a shows the trajectory of the vehicle's centre of gravity.

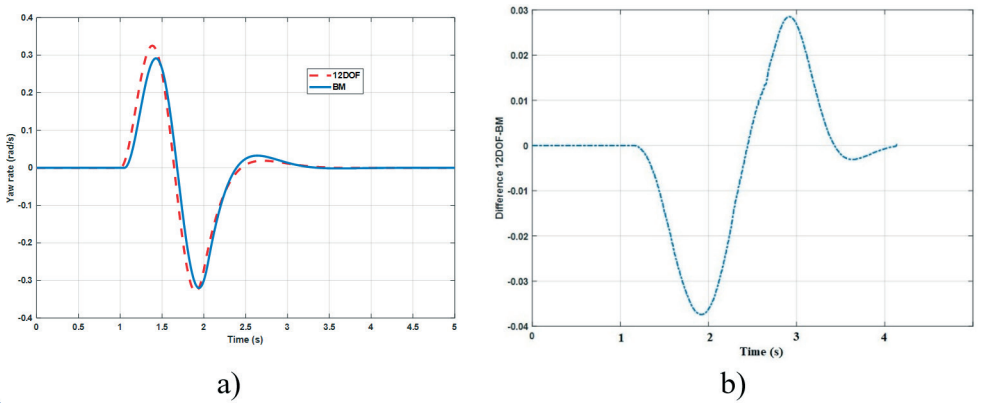

Fig. 10. Single lane change results (a) and difference 12DOF & BM (b): speed is 20 m/s

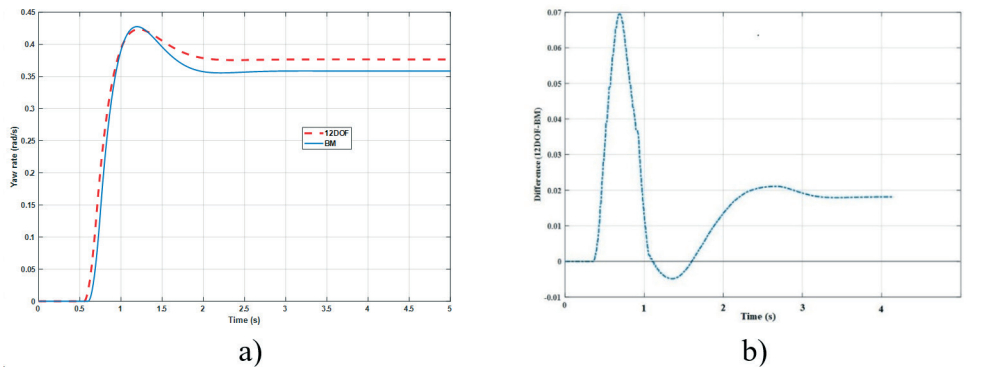

Fig. 11. J-turn results (a) and difference 12DOF & BM (b): speed is 20 m/s and the lane radius is 50 m

https://doi.org/10.14669/AM/192666

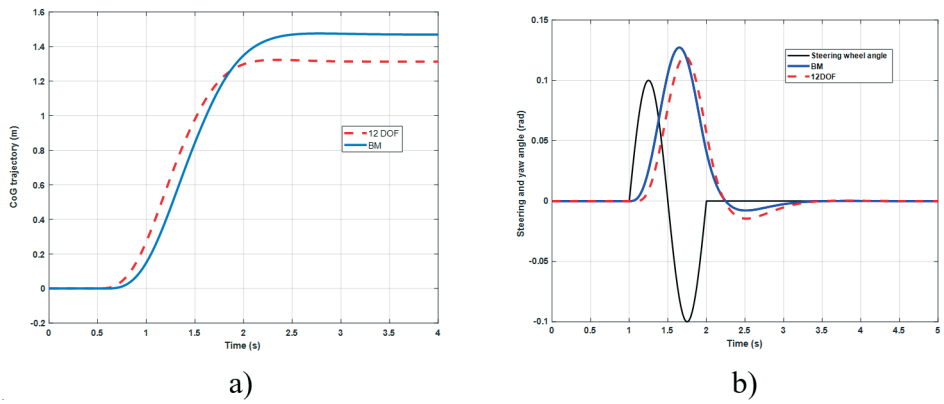

a) b)

Fig. 12. Single lane change results

4. Discussion

A comparative analysis of the '12DOF' and the corresponding experimental results revealed an initial discrepancy of (6–8)% in the recorded peak amplitude of the vertical displacement of the body (Figure 8a). The "Vertical BM" exhibited an error rate of (14–18)% in the experimental setting. It is noteworthy that the discrepancy between the 12DOF and experimental results increased by 10% in subsequent oscillation periods (Figure 8b). Similarly, when analysing the vibration of the body along the longitudinal axis, a discrepancy of (6–7)% was observed between the "12DOF" and experimental results in the initial "peak", with an error of (8–10)% noted in subsequent periods of vibration. The main reason for the observation of such an error is that the contact surface of the tire is considered as a point, that is, it is not considered as an occupied surface. Also, longitudinal and vertical deformations obtained from the vertical displacement of the tire at this point were not taken into account.

A discrepancy of 12DOF was observed in the angular velocity of the vehicle throughout the lane adjustment, with the experimental mean hovering around (9–10)%. Moreover, a discrepancy of (12–14)% was observed between the calculated and experimental values for the body mass (BM). The influence of the vehicle's suspension kinematics on the inclination angle of the wheel during manoeuvres has not been considered. Upon analysis of the J-turn results (as illustrated in Figure 9b), it was determined that the 12DOF experiment exhibited an average error of (6–7)%. The discrepancy between the theoretical and experimental outcomes can be attributed to the vertical loads exerted by the vehicle.

The discrepancy between the experimental results and the 'BM' model was found to be in the range of (13–15)%. It is worthy of note that in the 'BM' model, the discrepancy in the results increases when the speed exceeds 60 km/h and the lateral acceleration is greater than

https://doi.org/10.14669/AM/192666

4 m/s². The maximum discrepancy between the two models is 0.04 rad/s at a velocity of 20 m/s.The discrepancy between the 12DOF and BM modelling approaches is illustrated in Figure 11b, with a maximum difference of 0.07 rad/s. The results of the BM model were observed to be delayed by 0.3 seconds. Figure 12b illustrates the steering wheel turning angle and the yaw angle values for both models. The difference in modelling between 12DOF and BM was 0.22 m, with a maximum difference of 0.02 rad. To analyse the all-graphical results with the experiments and theoretical models that have been developed to explain the discrepancy between the current data point and the results obtained by deploying the MATLAB software.

Conclusions

Based on reviewed theoretical and experimental research, it is appropriate to use complete models when modelling car traffic on uneven roads, as well as single lane change and J-turn maneuvers. Analysis of real experiments shows that the vertical displacement of the vehicle body (sprung mass) over a single bump exhibits an error of (6–8)% in the initial peak amplitude. The error increases to (14–18)% when analyzing the 'Vertical BM' results. Additionally, it is observed that the error between the 12DOF and experimental results increases by 10% in subsequent oscillation periods. When analyzing the vibration of the body along the longitudinal axis, the experimental results showed a difference of (6–7)% in the initial peak and (8–10)% in the later periods of vibration compared to the 12DOF results. This difference can be attributed to the fact that 12DOF considers the moments of inertia in the Y-axis and the vibrations in this axis.

In the single lane change maneuver, the average error between 12DOF and experimental results was (9–10)%. Meanwhile, the error between 'BM' and the experiment was (12–14)%. This discrepancy can be attributed to the fact that the angle of wheel introduction resulting from suspension kinematics during the car's turn was not considered. Upon analyzing the J-turn results, the average error between the experimental results and 12DOF was (6–7)%. The difference between the 'BM' model and the experiment was (13–15)%. The 'BM' model showed an increase in error as the speed exceeded 60 km/h and the lateral acceleration exceeded 4.5 m/s². The experimental error was close to 15% when the speed of movement increased from (75–80) km/h in the 12DOF model, likely due to the linearity of the tire model. This is due to the non-linear elastics of the steering and suspension, as well as the kinematic introduction during the turn of the car. Based on the conducted research, it is recommended to use non-linear models of tires and suspensions in further studies.

The 12DOF model and modeling method described above can be used to control and predict traffic stability in the 'car–driver' system at low speeds.

5. Acknowledgement

This research has been funded by the Government's project №AB-V-2019.

6. Nomenclature

CoG	center of gravity
BM	2 degrees of freedom
Vertical BM	3 degrees of freedom 'vertical bike model'
12DOF	12 degrees of freedom full model

7. References

[1] Choi M, Moon C. Development of coordinator for optimal tireforces distribution for vehicle dynamics control considering nonlinear tire characteristics. International Journal of Automotive Technology. 2024;25(3):689–698. https://doi.org/10.1007/s12239-024-00054-2.

[2] Fathi H, El-Sayegh Z, Ren J, El-Gindy M. Modeling and Validation of a Passenger Car Tire Using Finite Element Analysis. Journal of Vehicles. 2024;6(1):384–402. https://doi.org/10.3390/vehicles6010016.

[3] Riva G, Formentin S, Corno M, Savaresi SM. Twin-in-the-loop state estimation for vehicle dynamics control: Theory and experiments. IFAC Journal System Control. 2024;29(100274):100274. https://doi.org/10.1016/j.ifacsc.2024.100274.

[4] Yaakoubi H, Haggège J, Rezk H, Al-Dhaifallah M. Explicit hybrid MPC for the lateral stabilization of electric vehicle system. Energy Reports. 2024;11:1100–1111. https://doi.org/10.1016/j.egyr.2023.12.066.

[5] Jaafari SMM, Shirazi KH. Integrated vehicle dynamics control via torque vectoring differential and electronic stability control to improve vehicle handling and stability performance. The Journal of Dynamic Systems, Measurement, and Control. 2018;140(7):071003:112–125. https://doi.org/10.1115/1.4038657.

[6] Abe M, Mokhiamar O. An integration of vehicle motion controls for full drive-by-wire vehicle Proceedings of the Institution of Mechanical Engineers, Part K: Journal of Multi-body Dynamics. 2007;221(1):116–127. https://doi.org/10.1243/14644193jmbd72.

[7] Yun S, Lee J, Jang W, Kim D, Choi M, Chung J. Dynamic modeling and analysis of a driving passenger vehicle. Applied Sciences. 2023;13(10):5903. https://doi.org/10.3390/app13105903.

[8] Zeping F, Jianmin D. Optimal Lane change motion of intelligent vehicles based on extended adaptive pseudo-spectral method under uncertain vehicle mass. Advances in Mechanical Engineering. 2017;9(7):168781401770282. https://doi.org/10.1177/1687814017702823.

[9] Zhu B, Chen Y, Zhao J, Su Y. Design of an integrated vehicle chassis control system with driver behavior identification. Mathematical Problems Engineering. 2015;2015:954514. https://doi.org/10.1155/2015/954514.

[10] Ikenaga S, Lewis FL, Campos J, Davis L. Active suspension control of ground vehicle based on a full-vehicle model. Proceedings of the 2000 American Control Conference. 2000;6:4019–4024. https://doi.org/10.1109/ACC.2000.876977.

[11] Ricco M, Alshawi A, Gruber P, Dhaens M, Sorniotti A. Nonlinear model predictive control for yaw rate and body motion control through semi-active and active suspensions. Vehicle System Dynamics. 2024;62(6):1587–1620. https://doi.org/10.1080/00423114.2023.2251615.

[12] Mazzilli V, De Pinto S, Pascali L, Contrino M, Bottiglione F, Mantriota G, et al. Integrated chassis control: Classification, analysis and future trends. Annual Reviews in Control. 2021;51:172–205. https://doi.org/10.1016/j.arcontrol.2021.01.005.

[13] Park K, Heo SJ, Kang DO, Jeong JI, Yi JH, Lee JH, et al. Robust design optimization of suspension system considering steering pull reduction. The International Journal of Automotive Technology. 2013;14(6):927–933. https://doi.org/10.1007/s12239-013-0102-3.

[14] Guo L, Ge P-S, Yue M, Zhao Y-B. Lane changing trajectory planning and tracking controller design for intelligent vehicle running on curved road. Mathematical Problems Engineering. 2014;2014:1–9. https://doi.org/10.1155/2014/478573.

[15] Antonov DA. Teoriya ustoychivosti dvizheniya mnogoosnykh avtomobiley. Moscow. Mashinostroenie, 1978. (Russian)

[16] Yoshida H, Shinohara S, Nagai M. Lane change steering manoeuvre using model predictive control theory. Vehicle System Dynamics. 2008;46:669–681. https://doi.org/10.1080/00423110802033072.

[17] Chan PT, Rad AB, Ho ML. A study on lateral control of autonomous vehicles via fired fuzzy rules chromosome encoding scheme. Journal of Intelligent and Robotic Systems. 2009;56(4):441–467. https://doi.org/10.1007/s10846-009-9330-1.

[18] Hatipoglu C, Ozguner U, Redmill KA. Automated lane change controller design. IEEE Transactions on Intelligent Transportation Systems. 2003;4(1):13–22. https://doi.org/10.1109/TITS.2003.811644.

[19] Yu F, Li D-F, Crolla DA. Integrated Vehicle Dynamics Control —state-of-the art review. 2008 IEEE Vehicle Power and Propulsion Conference. 2008;4677809. https://doi.org/10.1109/VPPC.2008.4677809.

[20] ISO 3888-2:2002 Passenger cars – Test track for a severe lane-change manoeuvre – Part 2: Obstacle avoidance.